



ACCEPTED MANUSCRIPT

## Development of the relativistic runaway avalanches in the lower atmosphere above mountain altitudes

To cite this article before publication: Ashot Chilingarian *et al* 2022 *EPL* in press <https://doi.org/10.1209/0295-5075/ac8763>

### Manuscript version: Accepted Manuscript

Accepted Manuscript is “the version of the article accepted for publication including all changes made as a result of the peer review process, and which may also include the addition to the article by IOP Publishing of a header, an article ID, a cover sheet and/or an ‘Accepted Manuscript’ watermark, but excluding any other editing, typesetting or other changes made by IOP Publishing and/or its licensors”

This Accepted Manuscript is © 2022 EPLA.

During the embargo period (the 12 month period from the publication of the Version of Record of this article), the Accepted Manuscript is fully protected by copyright and cannot be reused or reposted elsewhere.

As the Version of Record of this article is going to be / has been published on a subscription basis, this Accepted Manuscript is available for reuse under a CC BY-NC-ND 3.0 licence after the 12 month embargo period.

After the embargo period, everyone is permitted to use copy and redistribute this article for non-commercial purposes only, provided that they adhere to all the terms of the licence <https://creativecommons.org/licenses/by-nc-nd/3.0>

Although reasonable endeavours have been taken to obtain all necessary permissions from third parties to include their copyrighted content within this article, their full citation and copyright line may not be present in this Accepted Manuscript version. Before using any content from this article, please refer to the Version of Record on IOPscience once published for full citation and copyright details, as permissions will likely be required. All third party content is fully copyright protected, unless specifically stated otherwise in the figure caption in the Version of Record.

View the [article online](#) for updates and enhancements.

# Development of the relativistic runaway avalanches in the lower atmosphere above mountain altitudes

A.Chilingarian, G.Hovsepyan, T.Karapetyan, B.Sargsyan, and M.Zazyan

*A. Alikhanyan National Lab (Yerevan Physics Institute), Alikhanyan Brothers 2, Yerevan, Armenia, 0036*

## Abstract

The comparative analysis of three thunderstorms on Aragats in May 2021 demonstrates that relativistic runaway electron avalanches (RREAs) can reach very low altitudes above the earth's surface on mountain altitudes. Reaching the earth's surface RREAs are registered by the particle detectors as thunderstorm ground enhancements (TGEs) – large enhancements of electron and gamma ray fluxes, sometimes exceeding the fair-weather background fluxes up to a hundred times. By comparing the energy spectra of electrons and gamma rays it is possible to estimate the height above the ground where RREA terminates and avalanche particles exit the accelerating field. For the several registered on Aragats TGEs, this estimate varied between 50 and 150 meters. The threshold electric field can reach  $\approx 2.0$  kV/cm on heights of  $\approx 3300$ . When a lightning's active zone is above particle detectors RREAs last tens of seconds to a few minutes, until lightning flashes terminate electron acceleration. If the lightning activity is far from the detector site, TGEs are extended for a few tens of minutes and smoothly decayed and TGE has a more or less symmetrical shape.

## Plain language summary

We introduce a novel method for remote sensing of atmospheric electric fields. Advanced particle spectrometers operated on the mountain altitudes on Aragats station are tuned for the measurement of energy spectra of charged and neutral particles separately. This gives possibility to estimate the strength of the electric field in the lower atmosphere and estimate the particle flux incident on the earth's surface from the most powerful natural electron accelerators. Huge fluxes of electrons and gamma rays can exceed the background up to 100 times and pose yet not estimated influence on the climate. The long-term effects of this radiation on humans should be also carefully estimated.

## Key points

1. The strong accelerating electric field can extend very low above the mountain altitudes, reaching  $\approx 2.0$  kV/cm at altitudes  $\approx 3300$  m, 50-150 m above the earth's surface;
2. During a large storm on Aragats on the first of May 2022 we registered TGEs coinciding in time at a distance of 12.8 km;
3. Long-lasting TGE continued both during positive and negative NSEF, demonstrating that particle acceleration with emerged LPCR and after its decay can be smoothly continued.
4. We observed an intense graupel fall during positive NSEF, which is evidence of the decay of the LPCR that is "sitting" on graupels.

## 1. Introduction

1  
2  
3 The atmospheric electric field not only initiates lightning flashes but also modulates traversing  
4 cosmic ray flux, greatly enhancing the electron and gamma ray fluxes. To reach a complete  
5 understanding of the atmospheric electric field we need to establish easily measured indicators of  
6 field profile and maximum strength. Huge fluxes of electrons, positrons, gamma rays originating  
7 in the thunderous atmosphere (so-called relativistic runaway electron avalanches, RREAs,  
8 Gurevich, et al., 1992, Babich, et al., 1999, Dwyer, 2003) are detected on the earth's surface as  
9 thunderstorm ground enhancements (TGEs, Chilingarian, et al., 2009, 2010). A free electron  
10 entering the strong and extended electric field accelerates and unleashes the relativistic runaway  
11 electron avalanches exceeding the background level of gamma rays and electrons sometimes up  
12 to a hundred times (Chum, et al., 2021). RREA is a threshold process, which occurred only if the  
13 electric field exceeds the threshold (critical) value in a region of the vertical extent of about 1–2  
14 km, allowing steady development of the electromagnetic avalanche. RREA development  
15 simulations (Chilingarian et al., 2021a) reveal the possibility of electron acceleration up to 50  
16 MeV in the strong and extended atmospheric electric fields above spectrometers.  
17  
18  
19

20  
21 The remote sensing of the strong electric fields is rather a difficult problem. Till now the balloon  
22 soundings provide the only available data to sample the entire depth of a storm. Between 1978  
23 and 2000, more than 250 instrumented balloons were launched into thunderstorms over the Great  
24 Plains and New Mexico mountains in the U.S (Marshall, et al., 2001) to measure in-cloud  
25 electric fields Based on these measurements scientists of Langmuir laboratory recover the  
26 altitude dependence of the atmospheric electric field during New Mexico Mountain  
27 thunderstorms. Of nine electric field altitude profiles discussed in (Stolzenburg, et al., 2007), five  
28 “show a rapid increase in E for 2–5 s before the nearby lightning flash”. In the Fig. 1a of  
29 (Stolzenburg, et al., 2007) the electric field just before the flash was 117% of the RREA  
30 threshold. However, balloon launches are rare and very slow (20-40 minutes to traverse a storm);  
31 they perform measurements along the uncontrolled and random flight path, and usually, balloons  
32 are taken away by the wind and/or occasionally destroyed by the lightning flash.  
33  
34

35  
36 At Aragats research station we develop a new approach for estimating the strength of the  
37 atmospheric electric field by measuring the energy spectra of TGE particles (Chilingarian et al.,  
38 2021a). The 24/7 monitoring of almost all species of secondary cosmic rays is going on near 15  
39 years. We simultaneously observe graupel fall, the outside temperature, the near-surface electric  
40 field, and neutral and charged particle count rates. Such a multisensory approach allows us not  
41 only to estimate huge particle fluxes incident the earth's surface but also to get insight into the  
42 atmospheric electric field strength.  
43

44  
45 It is widely accepted, that the cloud charge structure for a typical thunderstorm contains an upper  
46 positive charge region consisting of ice crystals, a main negative charge region consisting of  
47 graupel and snow, and a transient lower positive charge region consisting of graupel. The electric  
48 charge of graupel is positive at temperatures warmer than  $-10^{\circ}\text{C}$ , and negative at temperatures  
49 cooler than  $-10^{\circ}\text{C}$  (Takahashi, 1978, Wada et al., 2021). Review (Williams, 1989) stated that the  
50 tripolar structure of thunderstorms is supported by a wide variety of observations and that  
51 temperature appears to be the most important single parameter in controlling the polarity of  
52 charge acquired by the precipitation particles. When graupel falls into the region warmer than  $\approx -$   
53  $10^{\circ}\text{C}$ , a charge reversal will occur in the central part of the storm, and the graupel population  
54 will change the charge from negative to positive. A large and dense graupel population either  
55  
56  
57  
58  
59  
60

1  
2  
3 suspended in the middle of the thunderstorm cloud or falling toward the earth's surface  
4 constitutes a "moving" lower positive charge region (LPCR). The dipole formed by the transient  
5 LPCR and main negative (MN) charge region intensifies the electric field of the dipole formed  
6 by the MN and its mirror image in the ground (MN-MIRR, MN-LPCR see Fig.1 in Chilingarian  
7 et al., 2021b). After the graupel fall, or after the lightning flash consumes a positive charge of the  
8 LPCR, the surface electric field again is controlled by the main negative charge region only (see  
9 the detail of the RREA initiation model in (Chilingarian et al, 2020 and 2021b)).  
10  
11

## 12 **2. Comparative analysis of TGEs occurred on 23 - 25 May 2021**

13

14  
15 According to the adopted approach of the multivariate correlation analysis, we use as many as  
16 possible measurements for characterizing high-energy processes in the atmosphere. The count  
17 rate of electron and gamma ray fluxes, as well, as the energy release histograms, are registered  
18 by particle spectrometers allowing to recover of differential energy spectra of both charged and  
19 neutral fluxes (Aragats solar neutron telescope, ASNT, Chilingarian, et al., 2017a, Chilingarian,  
20 et al. 2022b). The lightning identification and distance to lightning flash estimation are done by  
21 the monitoring of disturbances of the near-surface electric field (NSEF) with the network of  
22 EFM-100 electric mills of BOLTEC company. Meteorological measurements are made with the  
23 DAVIS weather station. The moon-glow panoramic cameras are used for the monitoring of skies  
24 above Aragats and identifying the graupel fall (see section 5 of supplemental materials - SM).  
25 We use the atmospheric electricity sign convention, according to which the downward directed  
26 electric field or field change vector is positive.  
27

28  
29 On May 23, 2021, a large storm was unleashed just above the Aragats research station. Storm  
30 duration was 6 hours with more than a hundred nearby lightning flashes. NSEF shows many  
31 episodes of deep negative and deep positive (-20 - +20 kV/m) field excursions. The electric field  
32 direction reversals after lightning strikes were very fast (a few seconds). In the first part of the  
33 storm, numerous attempts to start TGE were registered. In Fig 1, we present a 20-minute period  
34 of the thunderstorm with 2 TGEs terminated by lightning flashes on the initial stage of  
35 development, denoted in Fig. 1 by green arrows. The flashes occurred at 15:10:29 (distance to  
36 lightning flash was 1.7 km) and at 15:12:05 (distance to lightning flash was 5.7 km). The  
37 duration of TGEs was  $\approx 20$  sec, the NSEF was in the negative domain, and the amplitude of the  
38 NS field surge was  $\approx 50$  kV/m. The graupel fall continued during TGE. It is interesting to note  
39 that a new TGE started just after lightning terminates the previous one during the electric field  
40 recovering stage. This is evidence of the largely electrified atmosphere when a TGE opens the  
41 path to the lightning leader (Chilingarian et al., 2017b). In our first TGE classification according  
42 to NSEF disturbances (Chilingarian & Mkrtchyan, 2012, and section 6 of SM), this TGE falls  
43 into the fourth category, namely, "Multiple disturbances of a near-surface electrical field  
44 accompanied by numerous flashes of lightning".  
45  
46  
47  
48  
49  
50  
51  
52  
53  
54  
55  
56  
57  
58  
59  
60

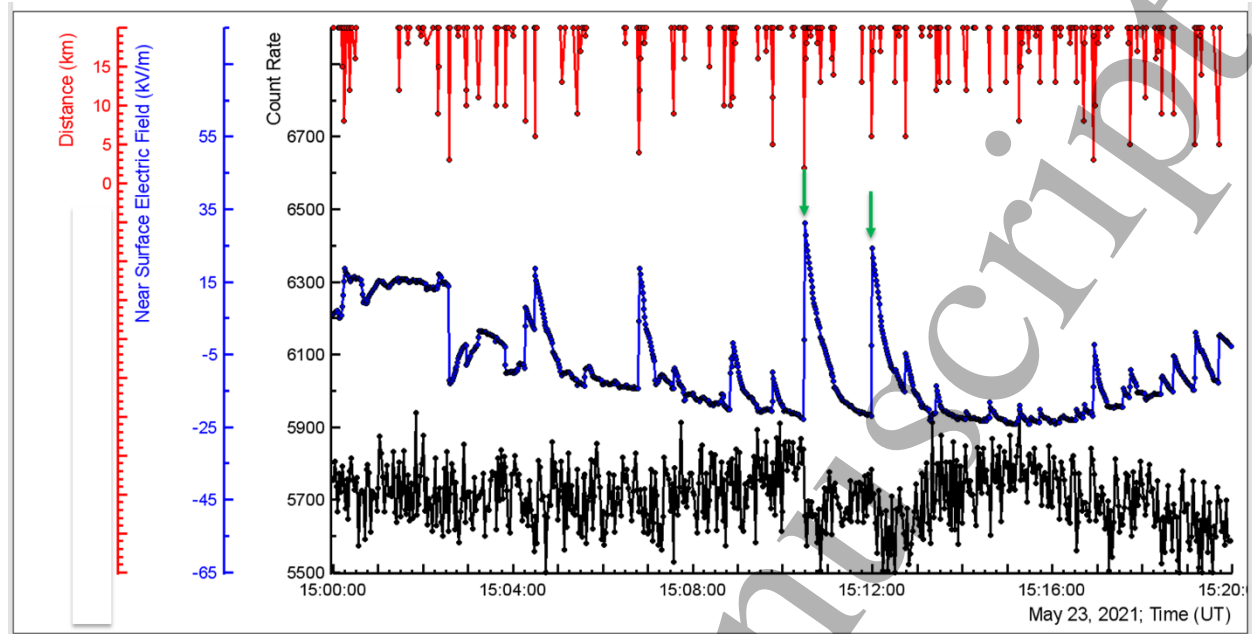


**Figure 1.** A pattern of the progress of the storm on Aragats on 23 May. Disturbances of the NS electric field (blue); count rate of ASNT spectrometer (black); and distances to lightning flashes (red lines). By green arrows, we show lightning flashes terminated starting TGEs.

During the second storm that occurred the next day on May 24 and lasted for 3 hours (see Fig. 2), the electrification of the atmosphere above the station was smaller. The nearby lightning flashes occurred only during the first 15 minutes of the storm terminating several small TGEs, analogically to ones that occurred on the previous day. During the large TGE started at  $\approx 14:32$ , the nearest lightning flash was at a distance of more than 15 km, consequently, it did not disturb the smooth evolution of long duration ( $\approx 12$  minutes, denoted in Fig. 2 by green lines) intense TGE with the enhancement of  $\approx 13\%$  above the background value that was measured on fair weather before the storm.

The NSEF at the ground beneath a decaying thunderstorm at the start of TGE was in the positive domain  $\approx 5$  kV/m dominated by a positive charge overhead, in  $\approx 3$  minutes electric field reversal occurred and the NSEF was for  $\approx 10$  minutes deeply negative  $\approx -20$  kV/m. Such a TGEs occurred after the active phase of the storm when the distance to lightning flashes is larger than 8-10 km and TGE finished smoothly without being terminated by a lightning flash.

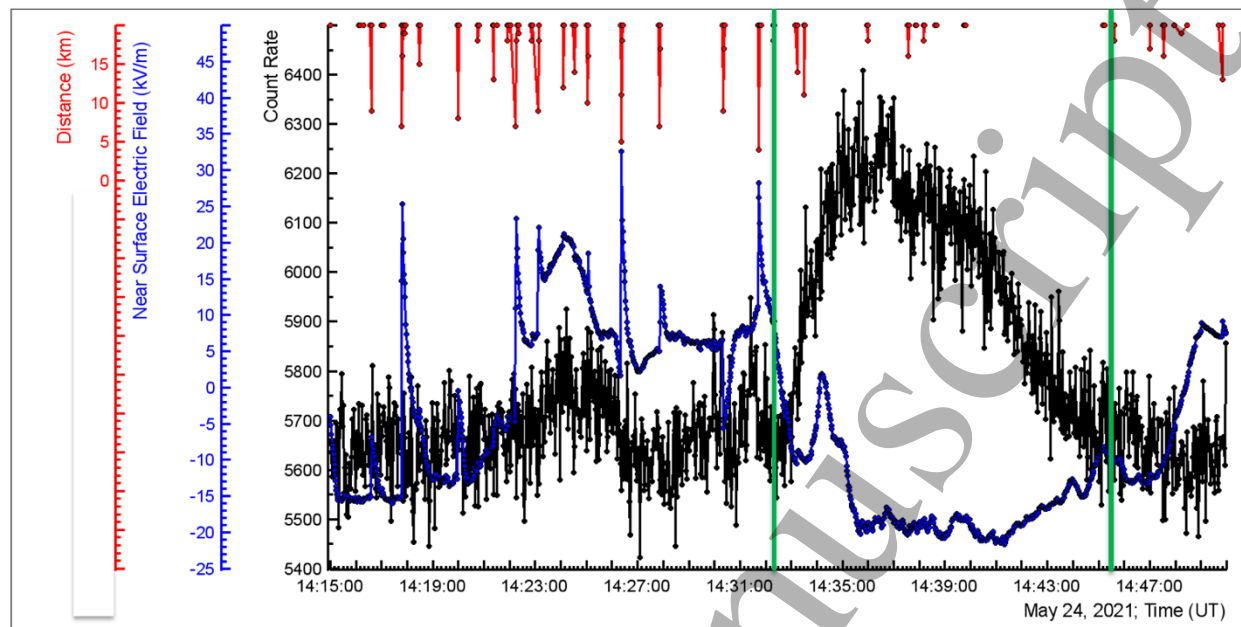


**Figure 2. Disturbances of the NS electric field (blue), count rate of ASNT spectrometer (black), and distances to lightning flashes (red). By the vertical green lines, we outline  $\approx 12$  minutes of TGE duration accompanied by the graupel fall.**

The TGE occurred on May 24 was considerably large and allowed recovery of the electron and gamma ray energy spectra (see criteria of the “electron” TGE selection in the first section of the SM). Energy spectra were approximated by the power-law dependence, parameters of which are posted in Table 1. In the second and third columns we show the power-law fit indices for the electron and gamma ray spectra; in the fourth and fifth the integral energy spectrum of both fluxes for energies larger than 7 MeV; in the sixth – the electron-to-gamma ray ratio; in the seventh and eighth – maximal energies of differential energy spectra for both species; and in the last – an approximate estimate of termination height of the strong accelerating electric field. The power-law indices were roughly constant during 8 minutes of the TGE mature phase and equal to  $\approx 2.0$  for electron spectrum, and  $\approx 2.4$  – for gamma ray spectrum.

As is expected due to large ionization losses of electrons the intensities and maximal energies of the electron flux are smaller than the same parameters of the gamma ray flux. However, the proximity of maximal energies of both TGE species demonstrates that the strong accelerating electric field in the atmosphere was rather low above the earth’s surface. The electron-to-gamma ray ratio is a very good indicator of the strong electric field height, the larger this ratio, the smaller the height of the strong accelerating electric field above the earth’s surface. At the exit from the strong electron accelerating electric field, the electron flux attenuates very fast and if this height is larger than 200 m practically it is impossible to recover the electron energy spectrum. For the heights above 200 m, the TGEs are dominated by the gamma ray flux, which is much more intensive than the electron flux. The gamma ray beam, on its travel to the earth’s surface, generates a small amount ( $\approx 1\%$  for energies larger than 7 MeV, see section 3 of SM), of electrons, born in the various electromagnetic interaction with the air, however, the methodology

of the of electron spectra recovery (see section 1 of SM and Chilingarian et al., 2022) rejects these TGEs as candidates to electron spectra recovery.

**Table 1. Main characteristics of the energy spectra of the TGE event for 8 minutes of the maximum TGE flux measured on 24 May 2021.**

Time	Power index Electr.	Power index $\gamma$	Number of Electrons with energy $>7\text{MeV}$	Number of Gamma rays with energy $>7\text{MeV}$	Ne/N $\gamma$ E $>7\text{MeV}$	E $_{\text{max}}$ electrons	E $_{\text{max}}$ gamma rays	H(m)
14:34	1.91	2.42	8.23E+02	6.98E+03	0.12	24	30	60
14:35	2.02	2.35	9.16E+02	9.27E+03	0.10	29	42	100
14:36	1.88	2.3	1.53E+03	8.58E+03	0.18	27	28	36
14:37	1.72	2.36	1.29E+03	7.72E+03	0.17	29	34	58
14:38	1.95	2.42	1.64E+03	7.24E+03	0.23	27	31	54
14:39	1.62	2.44	1.64E+03	6.66E+03	0.25	27	31	54
14:40	1.52	2.42	1.69E+03	6.80E+03	0.25	27	28	33

We can see in Table 1 rather large values of the electron-to-gamma ray ratio, corresponding to low locations of the strong electric field above the earth's surface. The distance where the strong accelerating field is terminated was calculated by the simple equation (Chilingarian et al., 2021d):

$$H = (1.2 * E_{\text{max}}^{\gamma} - E_{\text{max}}^{\text{e}}) / 0.2 \quad (1),$$

where we use estimated the height in meters, maximum energies of the electron and gamma ray flux in MeV and mean ionization losses of electron on altitudes 3000-5000 m assumed to be 0.2 MeV every meter. Selection of the coefficient 1.2, is based on the RREA propagation simulation, on the exit from the electric field, the maximum energies of electron flux are  $\approx 20\%$  larger than gamma ray maximum energies. Also, we assume that maximum energy gamma ray does not change significantly traversing 150 m or less in the atmosphere.

In Fig. 3a we show the histogram of the H values, calculated by eq. 1 for the collection of the "electron" TGEs posted in the Mendeley data set (Chilingarian and Hovsepyan, 2021). The mean value of estimates is slightly below 100 m and the standard deviation is 42 m. In Fig 3b we show the scatter plot of H with Ne/N $\gamma$ . As we can see, parameters correlated rather well and, therefore, usage of the approximate equation 1 is justified.

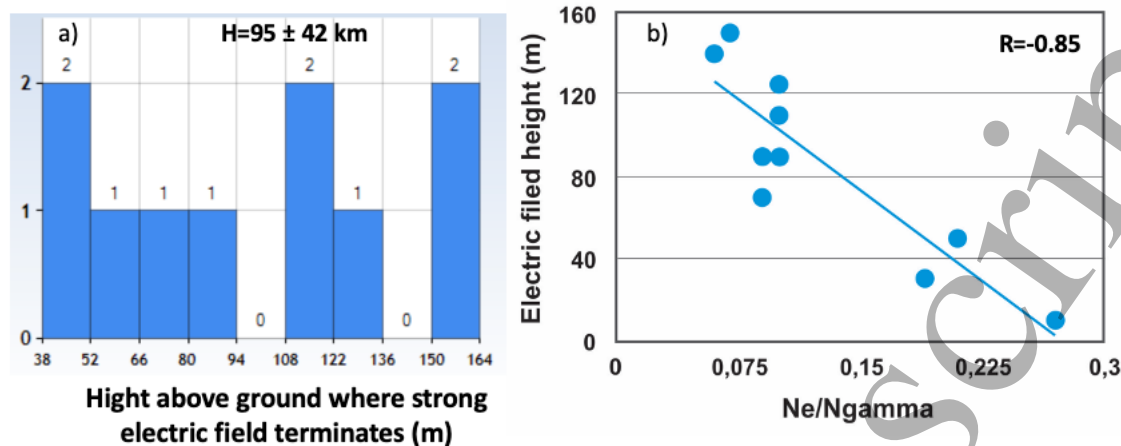


**Figure 3. a) The histogram of heights above ground where the strong accelerating field is terminated (H) obtained according to eq. 1; b) the H -Ne/N $\gamma$  scatter plot (for energies >7 MeV)**

The procedure of the estimation of the height where the strong accelerating electric field is terminated, in spite of the very simple equation (1), contains rather sophisticated procedures for the electron and gamma ray energy spectra recovering. These procedures included multiple generations of the electron-gamma ray avalanches with prechosen parameters i.e., RREA generation in the atmosphere, calculation of the detector response (transition from “theoretical” RREA to the “measured” TGE), and finally inverse problem solution (recovering of the RREA from the measured TGE). For checking the method’s accuracy, we made simulations with CORSIKA code corresponding to different strengths of the electric field and various heights of its termination. By applying to obtained “pseudo-experimental” samples all procedures used in the experimental data analysis chain, we obtain estimates of maximum energies of the electrons and gamma rays, as we do for the experimental data. After calculating the H parameter, we compare it with the corresponding “true” value that was chosen in the simulation trials. The final estimate of the standard error of H from these calculations was  $\approx 50$  m (see Table 1 of SM).

Development and decay of the LPCR are controlled by the graupel movement in the atmosphere and by the changing temperature profile (Kuettnner, 1950, Williams, 1989). When LPCR fully screens the detector’s site we observe a positive NSEF; when LPCR decays the surface detectors are exposed to the charge of the main negative (MN) layer, and, if this charge is sufficiently large TGE continued and reaches large intensities. Sure, LPCR does not screen the MN all the time, there can be several mixed cases (Nag & Rakov, 2009). The falling graupel appears with the start of the NS electric field reversal and with the TGE start, the graupel decline – with the TGE flux decay. The same behavior of the NSEF, with the graupel fall, is typical for the storms on the Tibetan plateau in China (Que et al.2005, Zhang et al., 2018). We can assume that the charge sitting on the graupel is reversed from the negative sign to the positive when the graupel has grown big at temperatures larger than  $-10^{\circ}\text{C}$ , or even larger than  $-15^{\circ}\text{C}$  (Takanashi, 1978, Berdeklis and List, 2001). TGEs occurred on Aragats mostly at surface temperatures  $-2^{\circ}\text{C}$  to  $+2^{\circ}\text{C}$ , thus, using an adiabatic lapse rate ( $-9.8^{\circ}\text{C}$  per 1 km) we come to an estimate of the possible LPCR charge reversal height of 1-1.5 km above the ground where temperatures reach a freezing level of  $-10^{\circ}\text{C}$  to  $-15^{\circ}\text{C}$ . The strong electric field can be extended low, below 200 m when the falling

positively charged graupel is “lowering” the “plate of the capacitor” (Kuettnner, 1950), Chilingarian, et al., 2021c, Wada, et al., 2021). Thus, the vertical extent of the accelerating field is not stable and completely decays with graupel fall. On 24 May, the duration of TGE coinciding with graupel fall was 12 minutes, in agreement with 1-1.5 km LPCR vertical size, if we assume 0.1-0.2 km/min graupel fall speed (Vázquez-Martín, et al., 2021).

On 25 May during a 1-hour long storm (the first category according to classification introduced in Chilingarian and Mkrtychyan, 2012, Fig. 5 and section 6 of SM), no nearby lightning flashes were registered at all. As we see in Fig. 4 TGE was lengthy, its duration was  $\approx 18$  minutes and particle flux continued both during positive and negative NSEF, demonstrating that particle acceleration with emerged LPCR and after its decay can be smoothly continued. It is worth noticing an intense graupel fall during positive NSEF, which is evidence of the decay of the LPCR that is “sitting” on graupels. During positive NSEF there were distant lightning flashes ( $>10$  km), during positive NSEF – the frequency of distant flashes highly diminished.

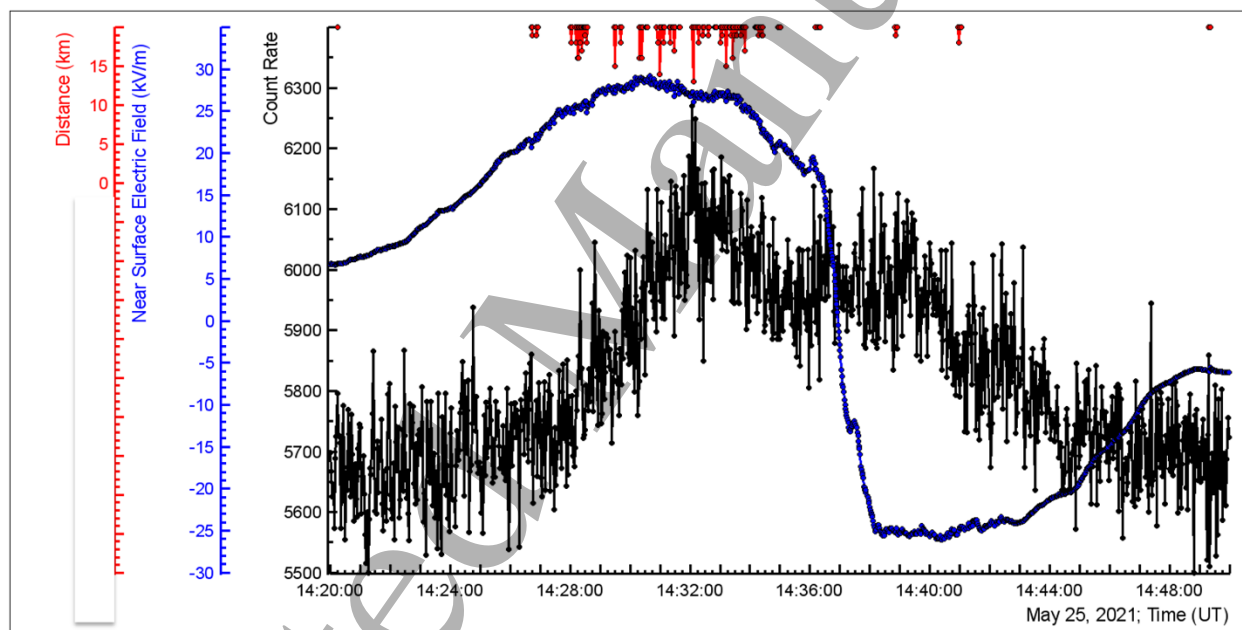


**Figure 4. A pattern of the progress of the storm on Aragats on 25 May. Disturbances of the near NS electric field (blue), count rate of ASNT spectrometer (black), and distance to lightning (red lines).**

### 3. Large scale horizontal atmospheric electric field

Monitoring of TGEs on slopes of Mt. Aragats gives clues to understanding the horizontal extension of the electric field, which supports RREA development above. The size of the particle emitting region in a thundercloud still remains not well researched. Measurements with multiple dosimeters installed at nuclear power plants in a coastal area of the Japanese sea made it possible to follow the source of the gamma ray flux moving with an ambient wind flow (Torii et al., 2011). At Nor Amberd research station, located on slopes of the Mt. Aragats at 2000 m height, the size of the particle emitting region was estimated Using the muon stopping effect

(Chilingarian et al., 2013, Chilingarian et al., 2021c). Estimates from both studies locate particle emitting regions within 1 km. However, in the recent radar-based gamma glow (TGE) study along the coast of the Japanese sea, it was observed that all TGEs were accompanied by the graupel fall, indicating the low location of the lower positively charged region (Wada et al., 2021). A strong radar echo due to the high reflectivity of hydrometeors indicates that the vertical and horizontal extent of the strong accelerating electric field was larger than 2 km. In another observation of the gamma glow in Japan, the flux enhancements were initiated and terminated exactly at the same time at a distance of 1.35 km (Hisadomi et al., 2021). Thus, the previously estimated values of particle emitting region size within 1 km seem to be highly underestimated.

Using a network of STAND1 particle detectors (Chilingarian et al, 2022a) we measure 50 ms and 1s time series of count rates of identical detectors during large enhancements of the particle intensity. The scatter plots demonstrate that near-surface electric field (NSEF) is rather uniform and stable during TGE at least on the high land where Aragats station is located (maximal distance between detectors is 300 m, see Fig. 20 of SM).

To get insight into the distribution of the atmospheric field at larger distances we establish networks of NaI spectrometers and electric field sensors of the EFM-100 type on the slopes of Mt. Aragats.

During a large storm on the first of May 2022, NSEF disturbances occurred both on Aragats and in Nor Amberd, reflecting the huge sizes of the storm. The storm started in Nor Amberd at 12:00 and on Aragats a few minutes later (start of disturbances of the NSEF) and finished at  $\approx$ 14:00. During the storm TGEs were observed both on Aragats and in Nor Amberd, see Fig.6. On Aragats we use 60 cm thick and 4 m<sup>2</sup> area scintillation spectrometer ASNT, and in Nor Amberd  $\approx$ 100 times smaller NaI spectrometer. Both detectors are located under a 0.8 mm iron roof and register gamma rays and electrons with energies above 4 MeV. The significance of the largest peak observed in Nor Amberd was 9%, corresponding to  $12\sigma$ . The significance of the first peak on Aragats at 13:01 was 3.7%, corresponding to  $9\sigma$ , and, of the second peak, not seen in Nor Amberd, on 13:30 – 8%, corresponding to  $20\sigma$ , see Figs 24 and 25 of SM. Although there were no exact coincidences in TGE times, however, inside the huge thundercloud above Aragats mountain slopes, simultaneously, for a few tens of minutes electron accelerator sends high-energy avalanche particles in direction of the earth's surface. Sure, we check the TGEs also by other particle detectors, on Aragats with solar neutron telescope, NaI spectrometer, 1 and 3 cm thick plastic scintillators, and in Nor Amberd with a tray of Geiger counters located outdoors. All detectors measure approximately the same parameters of TGE.

The NSEF changes during TGE from -23 to 8 kV/m on Aragats, and from -25 to 25 kV/m in Nor Amberd. In Fig.5 we show disturbances of NSEF, distances to the lightning flashes, and 1-minute time series of count rates of Aragats, Fig 5a, and Nor Amberd Fig. 5b detectors. Large enhancements of the count rates occurred on Aragats at 13 – 13:14 and 13:23-13:33, in Nor Amberd at 12:30-13:23. The lightning active zone was far from Aragats, more than 15 km; a lot of flashes occurred nearby Nor Amberd, the nearest ones – at a distance of 1.5 km. The NSEF changes during TGE from -23 to 8 kV/m on Aragats, and from -25 to 25 kV/m in Nor Amberd. The TGE occurred on Aragats during the deep negative electric field, and in Nor Amberd during positive NSEF. Thus, in spite of rather different conditions of the NSEF disturbances, and different charge structures in the cloud above, the TGEs in both destinations, share the approximately same time and enhancement.

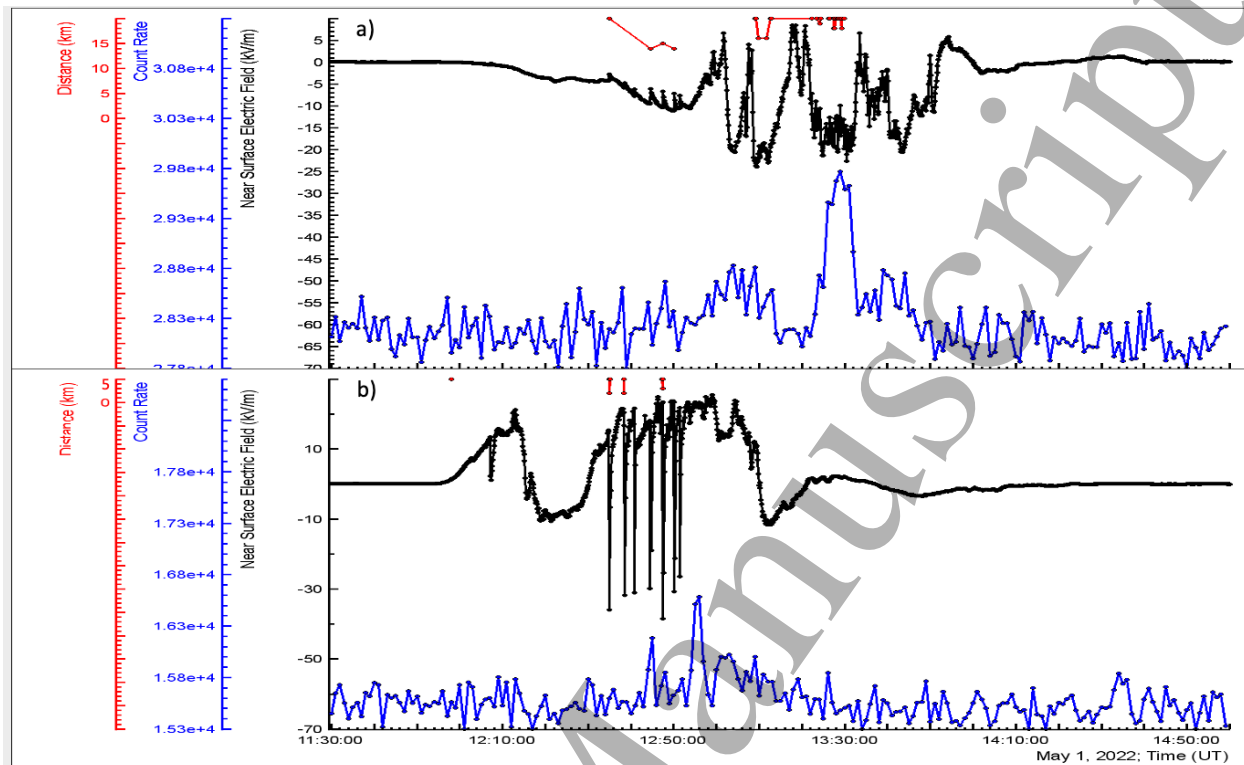


**Figure 5. The disturbances of the NSEF (black); 1-minute count rates of 5 cm thick and 1 m<sup>2</sup> area plastic scintillators (blue); and distances to lightning flashes (red) measured on Aragats a) and in Nor Amberd b).**

The orographic environment on Aragats and in Nor Amberd is rather different: Aragats is on high land near the mountain peaks, and Nor Amberd is on the mountain slope; thus, the thundercloud can be very low above Aragats, and rather high above Nor Amberd. Nonetheless, in spite of the different types of NSEF disturbances, and, different charge structures in the cloud above, the TGEs on Aragats and 12.8 km apart in Nor Amberd, occurred at the same time and demonstrate approximate coinciding maximum energies well above 10 MeV (see details in section 7 of SM).

#### 4. Discussion and conclusions

Remote sensing of electric fields in the lower atmosphere by measuring the energy spectra of electrons and gamma rays provides several advantages over balloon measurements. Remote sensing can be done on the earth's surface distant from the storm and does not require balloon launches near the most intense weather. Surface detectors are stable and long-leaving, they are not moved by wind or destroyed by lightning flash like balloons. Several detectors can monitor multiple regions of interest simultaneously. The time resolution is seconds, and not tens of minutes as for balloon flights, monitoring is performed 24/7, without a chance to miss interesting storms. We found that especially important is the diagnostic of the strong electric field just above the atmosphere with an accuracy of  $\approx 50$  m. The remote sensing of the atmospheric field can be used along with field mill climatology to minimize the risk of launching space vehicles during thunderstorms (Gardner, 2020).

1  
2  
3 By adding to the NSEF measurement, the information on electron and gamma ray energy  
4 spectra, the electric field structure in the lower part of the atmosphere can be characterized with  
5 more details.  
6  
7

8 3 episodes of electron acceleration observed at the end of May 2021 on Aragats demonstrate a  
9 rich variability of the electron accelerator operation modes depending on the proximity of the  
10 detection site to the active storm region and extension of the strong accelerating field relative to  
11 the earth's surface. LPCR is sitting mainly on precipitation (graupel) that becomes positively  
12 charged above  $\approx -10\text{C}^\circ$ . Thus, the falling LPCR elongates the accelerating field until very low  
13 heights above the ground and the electric field of the lower dipole accelerates electrons to high  
14 energies due to large potential differences. In the Spring season, almost every thunderstorm and  
15 TGE on Aragats was accompanied by a graupel fall which was monitored on a minute time  
16 scale. The TGEs occurred on 24-25 May are a good verification of the described above model.  
17 At the beginning of TGE, the graupel dipole cause the large positive NSEF, which was seen on  
18 May 25 (Fig 3). Several remote lightning flashes during the positive NSEF led to a field reversal  
19 and the NSEF falls in the deep negative domain, sustaining the second phase of TGE (no  
20 lightning flashes occurred during this phase).  
21  
22  
23

24 The estimates of the electron-to-gamma ray ratio and termination height of the strong electric  
25 field confirmed the low location of the electric field in good agreement with the TGE initiation  
26 model, and - with simulation results (Chilingarian et.al., 2020 and 2021b).  
27  
28

29 On the first of May 2022, a strong intracloud electric field initiated TGEs above research stations  
30 Aragats and Nor Amberd separated by a distance of 12.8 km. Thus, the RREA can be unleashed  
31 in the same time at a very large distance, reaching 10 km and more.  
32

### 33 **Data Availability Statement**

34  
35 The data for this study are available on the WEB page of the Cosmic Ray Division (CRD) of the  
36 Yerevan Physics Institute, <http://adei.crd.yerphi.am/adei> and from Mendeley data sets,  
37 Chilingaryan and Hovsepyan, 2021, Soghomonyan and Chilingarian, 2021).  
38  
39

### 40 **Acknowledgment**

41  
42 We thank the staff of the Aragats Space Environmental Center for the operation of the  
43 uninterrupted operation of all particle detectors and field meters. The authors thanks S.  
44 Soghomonyan for useful discussion. The authors acknowledge the support of the Science  
45 Committee of the Republic of Armenia, in the frames of the research project № 21AG-1C012.  
46  
47

### 48 **References**

49  
50 A. Chilingarian, A. Daryan, K. Arakelyan, et al., Ground-based observations of thunderstorm-  
51 correlated fluxes of high- energy electrons, gamma rays, and neutrons, Phys. Rev. D 82 (2010)  
52 043009.  
53  
54  
55  
56  
57  
58  
59  
60

1  
2  
3 A.Chilingarian, G. Hovsepyan, A. Hovhannisyan, Particle bursts from thunder- clouds: natural  
4 particle accelerators above our heads, *Phys. Rev. D* 83 (2011) 062001.  
5

6  
7 A Chilingarian, N Bostanjyan, T Karapetyan, On the possibility of location of radiation-emitting  
8 region in thundercloud, *IOP Publishing Journal of Physics: Conference Series* 409 (2013)  
9 012217 doi:10.1088/1742-6596/409/1/012217

10 Chilingarian A., Hovsepyan G., Mailyan B., 2017a, In situ measurements of the Runaway  
11 Breakdown (RB) on Aragats mountain, *Nuclear Inst. and Methods in Physics Research*, A  
12 874,19–27.  
13

14  
15 Chilingarian A., Chilingaryan S., Karapetyan T., et al., 2017b, On the initiation of lightning in  
16 thunderclouds, *Scientific Reports* 7, Article number: 1371, DOI:10.1038/s41598-017-01288-0.  
17

18 A.Chilingarian, G. Hovsepyan, S. Soghomonyan, M. Zazyan, and M. Zelenyy, Structures of the  
19 intracloud electric field supporting origin of long-lasting thunderstorm ground enhancements,  
20 *Physical review* 98, 082001(2018).  
21

22  
23 A. Chilingarian, G. Hovsepyan, T. Karapetyan, G. Karapetyan, L. Kozliner, H. Mkrtchyan, D.  
24 Aslanyan, and B. Sargsyan, Structure of thunderstorm ground enhancements, *Phys. Rev. D* 101,  
25 122004 (2020).  
26

27 A.Chilingarian, G. Hovsepyan, and M. Zazyan, Measurement of TGE particle energy spectra: An  
28 insight in the cloud charge structure, *Europhysics letters* (2021a), 134, 6901,  
29 <https://doi.org/10.1209/0295-5075/ac0dfa>.  
30

31  
32 A. Chilingarian, G. Hovsepyan, E. Svechnikova, and M. Zazyan, Electrical structure of the  
33 thundercloud and operation of the electron accelerator inside it, *Astroparticle Physics* 132  
34 (2021b) 102615 <https://doi.org/10.1016/j.astropartphys.2021.102615>.  
35

36  
37 A. Chilingarian, G. Hovsepyan, G. Karapetyan, and M. Zazyan, Stopping muon effect and  
38 estimation of intracloud electric field, *Astropart. Phys.* 124, 102505 (2021c).  
39

40 Chilingarian, Ashot; Hovsepyan, Gagik (2022), “Dataset for 16 parameters of ten thunderstorm  
41 ground enhancements (TGEs) allowing recovery of electron energy spectra and estimation the  
42 structure of the electric field above earth’s surface”, *Mendeley Data*, V3, doi:  
43 10.17632/tvbn6wdf85.3  
44 <https://data.mendeley.com/datasets/tvbn6wdf85/3>  
45

46  
47 A.Chilingarian, G. Hovsepyan, T.Karapetyan, et al., Multi-messenger observations of  
48 thunderstorm-related bursts of cosmic rays, *Journal of Instrumentation*, *JINST* 17 P07022  
49 (2022a).  
50

51 A.Chilingarian, G. Hovsepyan, T.Karapetyan, et al., Measurements of energy spectra of  
52 relativistic electrons and gamma-rays avalanches developed in the thunderous atmosphere with  
53 Aragats Solar Neutron Telescope, *JINST* 17 P03002 (2022b).  
54  
55  
56  
57  
58  
59  
60

1  
2  
3 J. Chum, R. Langer, J. Baše, M. Kollárik, I. Strhárský, G. Diendorfer, and J. Ruzs, Significant  
4 enhancements of secondary cosmic rays and electric field at high mountain peak during  
5 thunderstorms, *Earth, Planets Space* 72, 72 (2020).  
6

7  
8 Hisadomi, S., Nakazawa, K., Wada, Y., Tsuji, Y., Enoto, T., Shinoda, T., et al. (2021). Multiple  
9 gamma-ray glows and a downward TGF observed from nearby thunderclouds. *Journal of*  
10 *Geophysical Research: Atmospheres*, 126, e2021JD034543. [https://doi.](https://doi.org/10.1029/2021JD034543)  
11 [org/10.1029/2021JD034543](https://doi.org/10.1029/2021JD034543)  
12

13  
14 S.C.Gardner, using a field mill climatology to assess all lightning launch commit criteria, AFIT-  
15 ENV-MS-20-M-204, 2020.  
16

17  
18 Gurevich, A., Milikh, G., & Roussel-Dupre, R. (1992). Runaway electron mechanism of air  
19 breakdown and preconditioning during a thunderstorm. *Physics Letters A*, 165(5–6), 463–468.  
20 [https://doi.org/10.1016/0375-9601\(92\)90348-P](https://doi.org/10.1016/0375-9601(92)90348-P).  
21

22  
23 T. C. Marshall, M. Stolzenburg, Voltage inside and just above thunderstorms, *JGR*, 106, 4757  
24 (2001)

25  
26 Soghomonyan, Suren; Chilingarian, Ashot (2022), “Thunderstorm ground enhancements  
27 abruptly terminated by a lightning flash registered  
28 both by WWLLN and local network of EFM-100 electric mills.”, Mendeley Data, V1, doi:  
29 10.17632/ygvjzdx3w3.1 <https://data.mendeley.com/datasets/ygvjzdx3w3/1>  
30

31  
32 M. Stolzenburg, T. C. Marshall, W. D. Rust, E. Bruning, D. R. MacGorman, and T. Hamlin  
33 (2007), Electric field values observed near lightning flash initiations, *Geophys. Res. Lett.*, 34,  
34 L04804, doi:10.1029/2006GL028777

35  
36 Takahashi, T. (1978), Riming electrification as a charge generation mechanism in thunderstorms,  
37 *J. Atmos. Sci.*, 35, 1536–1548.

38  
39 Torii, T., Sugita, T., Kamogawa, M., Watanabe, Y., & Kusunoki, K.  
40 Migrating source of energetic radiation generated by thunderstorm ac-  
41 tivity. *Geophysical Research Letters*, 38 24 (2011).  
42

43  
44 Wada, Y., Enoto, T., Kubo, M., Nakazawa, K., Shinoda, T., Yonetoku, D., et al. (2021).  
45 Meteorological aspects of gamma-ray glows in winter thunderstorms. *Geophysical Research*  
46 *Letters*, 48, e2020GL091910. <https://doi.org/10.1029/2020GL091910>  
47 E.R. Williams, The tripole structure of thunderstorms, *JGR* 94 (1989) 151-13,167.

48  
49 Sandra Vázquez-Martín, Thomas Kuhn, and Salomon Eliasson, Shape dependence of snow  
50 crystal fall speed, *Atmos. Chem. Phys.*, 21, 7545–7565, 2021 [https://doi.org/10.5194/acp-21-](https://doi.org/10.5194/acp-21-7545-2021)  
51 [7545-2021](https://doi.org/10.5194/acp-21-7545-2021)  
52  
53  
54  
55  
56  
57  
58  
59  
60

1  
2  
3  
4  
5  
6  
7  
8  
9  
10  
11  
12  
13  
14  
15  
16  
17  
18  
19  
20  
21  
22  
23  
24  
25  
26  
27  
28  
29  
30  
31  
32  
33  
34  
35  
36  
37  
38  
39  
40  
41  
42  
43  
44  
45  
46  
47  
48  
49  
50  
51  
52  
53  
54  
55  
56  
57  
58  
59  
60

Accepted Manuscript